Response of Water Use Efficiency to Global Environmental Change Based on Output From Terrestrial Biosphere Models

Sha Zhou[1], Bofu Yu[2] (iD), Christopher R. Schwalm[3,4], Philippe Ciais[5], Yao Zhang[6] (iD), Joshua B. Fisher[7] (iD), Anna M. Michalak[8], Weile Wang[9] (iD), Benjamin Poulter[10] (iD), Deborah N. Huntzinger[11] (iD), Shuli Niu[12,13] (iD), Jiafu Mao[14] (iD), Atul Jain[15] (iD), Daniel M. Ricciuto[14] (iD), Xiaoying Shi[14], Akihiko Ito[16] (iD), Yaxing Wei[14], Yuefei Huang[1,17], and Guangqian Wang[1]

[1]State Key Laboratory of Hydroscience and Engineering, Department of Hydraulic Engineering, Tsinghua University, Beijing, China, [2]Australian Rivers Institute and School of Engineering, Griffith University, Nathan, Queensland, Australia, [3]Woods Hole Research Center, Falmouth, MA, USA, [4]Center for Ecosystem Science and Society, Northern Arizona University, Flagstaff, AZ, USA, [5]Laboratoire des Sciences du Climat et de l'Environnement, CEA CNRS UVSQ, Gif-sur-Yvette, France, [6]Department of Microbiology and Plant Biology, Center for Spatial Analysis, University of Oklahoma, Norman, OK, USA, [7]Jet Propulsion Laboratory, California Institute of Technology, Pasadena, CA, USA, [8]Department of Global Ecology, Carnegie Institution for Science, Stanford, CA, USA, [9]School of Natural Sciences, California State University, Monterey Bay, Seaside, CA, USA, [10]Institute on Ecosystems and Department of Ecology, Montana State University, Bozeman, MT, USA, [11]School of Earth Sciences and Environmental Sustainability and the Department of Civil Engineering, Construction Management, and Environmental Engineering, Northern Arizona University, Flagstaff, AZ, USA, [12]Synthesis Research Center of Chinese Ecosystem Research Network, Key Laboratory of Ecosystem Network Observation and Modeling, Institute of Geographic Sciences and Natural Resources Research, Beijing, China, [13]College of Resources and Environment, University of Chinese Academy of Sciences, Beijing, China, [14]Environmental Sciences Division and Climate Change Science Institute, Oak Ridge National Laboratory, Oak Ridge, TN, USA, [15]Department of Atmospheric Sciences, University of Illinois at Urbana-Champaign, Urbana, IL, USA, [16]Institute for Materials Research, Tohoku University, Sendai, Japan, [17]College of Ecological and Environmental Engineering, Qinghai University, Xining, China

Abstract Water use efficiency (WUE), defined as the ratio of gross primary productivity and evapotranspiration at the ecosystem scale, is a critical variable linking the carbon and water cycles. Incorporating a dependency on vapor pressure deficit, apparent underlying WUE (uWUE) provides a better indicator of how terrestrial ecosystems respond to environmental changes than other WUE formulations. Here we used 20th century simulations from four terrestrial biosphere models to develop a novel variance decomposition method. With this method, we attributed variations in apparent uWUE to both the trend and interannual variation of environmental drivers. The secular increase in atmospheric CO_2 explained a clear majority of total variation (66 ± 32%: mean ± one standard deviation), followed by positive trends in nitrogen deposition and climate, as well as a negative trend in land use change. In contrast, interannual variation was mostly driven by interannual climate variability. To analyze the mechanism of the CO_2 effect, we partitioned the apparent uWUE into the transpiration ratio (transpiration over evapotranspiration) and potential uWUE. The relative increase in potential uWUE parallels that of CO_2, but this direct CO_2 effect was offset by 20 ± 4% by changes in ecosystem structure, that is, leaf area index for different vegetation types. However, the decrease in transpiration due to stomatal closure with rising CO_2 was reduced by 84% by an increase in leaf area index, resulting in small changes in the transpiration ratio. CO_2 concentration thus plays a dominant role in driving apparent uWUE variations over time, but its role differs for the two constituent components: potential uWUE and transpiration.

1. Introduction

Terrestrial plants assimilate atmospheric CO_2 through photosynthesis, a process that is accompanied by water loss from leaves. The ratio between the two is water use efficiency (WUE). By linking carbon and water exchange processes between terrestrial ecosystems and the atmosphere, WUE has been recognized as an effective indicator to assess the responses of terrestrial ecosystem to global environmental changes (Niu et al., 2011). The atmospheric CO_2 concentration has increased by more than 100 ppm since preindustrial times and is predicted to be 421–936 ppm by the year 2100, depending on emission scenarios (Intergovernmental Panel on Climate Change (IPCC), 2013). As a result of the radiative forcing of CO_2,

Table 1
Definitions of Water Use Efficiency, Intrinsic Water Use Efficiency, Inherent Water Use Efficiency, and Underlying Water Use Efficiency at the Leaf and Ecosystem Scales

WUE formulations	Leaf level	Ecosystem level	Reference
WUE	WUE = A/T	WUE = GPP/ET	Farquhar and Richards (1984) Law et al. (2002)
Intrinsic WUE (iWUE)	iWUE = A/g_s	-	Osmond et al. (1980)
Inherent WUE (IWUE)	-	IWUE = GPP·VPD/ET	Beer et al. (2009)
Underlying WUE (uWUE) or apparent uWUE (uWUEa)	uWUE = A·$D^{0.5}$/T	uWUE or uWUEa = GPP·$VPD^{0.5}$/ET	Zhou et al. (2014, 2016)
Potential uWUE (uWUEp)		uWUEp = GPP·$VPD^{0.5}$/T	Zhou et al. (2016)

Note. Abbreviations: carbon assimilation (A), transpiration (T), stomatal conductance (g_s), gross primary production (GPP), evapotranspiration (ET), water vapor pressure difference between inner-leaf and the atmosphere (D), and atmospheric vapor pressure deficit (VPD).

other greenhouse gases and aerosols, the mean global surface temperature is projected to increase by 1.0–3.7°C by the end of the 21st century (2081–2100), depending on emission scenarios and climate models (IPCC, 2013). In addition, the global precipitation regime will change considerably, with substantial impacts on the carbon and water cycles in terrestrial ecosystems. Human-caused land use change and nitrogen deposition also exert effects on global carbon and water biogeochemical processes (Gerber et al., 2013; Sterling, Ducharne, & Polcher, 2013). All these environmental factors impact ecosystem WUE and will continue to change WUE in future, both individually and in concert with one another. Therefore, it is important to investigate the responses of terrestrial ecosystem WUE to these environmental changes.

Several definitions of WUE have been proposed to describe the carbon-water relationships at different spatial scales (Table 1). At the leaf scale, WUE is defined as the ratio of carbon assimilation over transpiration (Farquhar & Richards, 1984). This ratio is usually replaced with the ratio of gross primary productivity (GPP) over evapotranspiration (ET) when scaling up from the leaf to the ecosystem scale (Law et al., 2002). GPP and ET are greatly influenced by the vapor pressure deficit (VPD), such that a WUE formulation that links WUE to VPD, an inherent WUE (IWUE = GPP·VPD/ET) at the ecosystem scale was proposed by Beer et al. (2009). At the leaf scale, IWUE corresponds to the intrinsic WUE (iWUE) and measures the amount of carbon assimilated per unit of stomatal conductance (Osmond, Bjorkman, & Anderson, 1980). Although IWUE is more appropriate than WUE to describe the carbon and water exchanges via stomata, IWUE depends on the ratio of inner leaf over ambient partial pressure of CO_2 (C_i/C_a) that is assumed to be relatively constant under given environmental conditions. Zhou et al. (2014) showed that IWUE varies with C_i/C_a as VPD varies at the subdaily timescale. Thus, they introduced the concept of underlying WUE, given by uWUE = GPP·$VPD^{0.5}$/ET, by combining IWUE using the C_i/C_a versus VPD relationship from Lloyd and Farquhar (1994). uWUE is closely related to plant physiological regulation of CO_2 and water exchanges, given the stronger empirical relationship between GPP·$VPD^{0.5}$ and ET in uWUE than other formulations based on data from the AmeriFlux network (Zhou et al., 2014, 2015).

At the ecosystem scale, the GPP·$VPD^{0.5}$ versus ET relationship assumes that ET is dominated by transpiration (T), while evaporation from soil and canopy interception is fairly small by comparison. The ecosystem uWUE, or apparent uWUE (uWUEa), can be decomposed as a product of canopy uWUE, or potential uWUE (uWUEp), and T/ET (Zhou et al., 2016) (Table 1). uWUEp is identical to the uWUE at the leaf scale and is relatively invariable under steady state conditions for a given vegetation type. Thus, the variation in uWUEa can be attributed to variations in uWUEp and T/ET under changing environmental conditions. Understanding the responses of uWUEp and T/ET to environmental changes thus sheds light on the controlling factors of the dynamics of the carbon-water relationship and provides insight into future changes in the terrestrial hydrological cycle.

Several studies have looked at the responses of WUE and IWUE (or iWUE) to rising atmospheric CO_2, climate change, and other environmental drivers (Niu et al., 2011; Zhu et al., 2011). However, the responses of uWUE to environmental change have not been investigated, although uWUE was found to be a better indicator to describe the interrelationship between carbon uptake and water losses at the AmeriFlux sites located in the U.S. (Zhou et al., 2015). Long-term increases in iWUE in response to the elevated CO_2 are consistent with measurements of tree ring isotopes in various forest species and sites (Andreu-Hayles et al., 2011; Battipaglia et al., 2013; Gagen et al., 2011; Levesque et al., 2014; Nock et al., 2011; Peñuelas, Canadell, & Ogaya, 2011). The increase in WUE and IWUE with rising atmospheric CO_2 is supported by flux tower measurements and simulations from process-based terrestrial ecosystem models (De Kauwe et al., 2013; Keenan et al., 2013; Knauer

et al., 2016). In comparison to WUE and iWUE, uWUE is more directly related to atmospheric CO_2 at the leaf scale, since uWUE can be expressed explicitly as a function of atmospheric CO_2, while WUE and iWUE are affected by both ambient and inner-leaf CO_2 concentrations (Zhou et al., 2014). The responses of uWUEa, which consist of the responses of uWUEp and T/ET, to atmospheric CO_2 are more complex at the regional and global scales. Several studies have indicated that vegetation responds to atmospheric CO_2 through changes in its physiology and structure (Betts et al., 1997; Kergoat et al., 2002; Piao et al., 2007). It is hypothesized that the ecosystem uWUEp and T/ET would concurrently respond to changes in the vegetation physiology (e.g., stomatal conductance) and ecosystem structure (e.g., leaf area index and vegetation type). Although the physiological and structural CO_2 effects on iWUE and T have been reported in previous studies (Frank et al., 2015; Saurer et al., 2014), these two effects have not been quantitatively estimated. Thus, separating the physiological and structural CO_2 effects on uWUEp and on T/ET can help better understand the responses of ecosystem uWUEa to the rising atmospheric CO_2 concentration.

In addition to atmospheric CO_2, uWUEa is also impacted by other drivers, including climate change, land use change, and nitrogen deposition, which affect both carbon uptake and water losses at the regional and global scales (Huang et al., 2015). Niu et al. (2011) indicated that ecosystem WUE responded negatively to climate warming but positively to increasing precipitation based on a 4 year manipulative field experiment in a temperate steppe in Northern China. But WUE may decrease or increase with increasing annual precipitation in different ecosystems, depending on water conditions and vegetation types (Tian et al., 2010). Land use change can directly impact ecosystem GPP and ET, and even alter regional carbon and water cycles (Kaplan, Krumhardt, & Zimmermann, 2012; Sterling et al., 2013). In addition, land use-related changes, for example, urbanization, deforestation, and afforestation, exert various impacts on regional uWUEa, resulting in spatial variations in the responses of uWUEa to land use change over the globe (Foley et al., 2005). In recent decades, human activities have brought considerable reactive nitrogen into terrestrial ecosystems around the world (Matson, Lohse, & Hall, 2002). For example, bulk nitrogen deposition has dramatically increased in China at a mean rate of 0.41 kg ha^{-1} yr^{-1} from 1980 to 2010, and foliar nitrogen increased by 32.8% on average for all plant species between the 1980s and 2000s (Liu et al., 2013). The increased foliar nitrogen concentration stimulates both GPP and ET and may change ecosystem uWUEa, especially for nitrogen-limited ecosystems (Guerrieri et al., 2016; Mitchell & Hinckley, 1993). Because uWUEa is affected by various drivers, it is important to separate the impacts of key drivers and quantify the contribution of each driver at the regional and global scales. While ecosystem models have been developed to describe and quantify the responses of carbon and water cycles to different environmental drivers (Huntzinger et al., 2013), outputs from these models have not yet been used in an attribution analysis of the trend and interannual variations in uWUEa. Results of this analysis could help postulate hypotheses to be tested with new observations.

The aim of this study is to investigate the responses of uWUEa to environmental changes over the globe during the period of 1901–2010. In order to isolate the effects of the four key drivers, that is, atmospheric CO_2, climate change (changes in seven climate variables), land use change, and nitrogen deposition, we analyzed results from four terrestrial biosphere models (TBMs) that simulated all four of these drivers in the Multi-scale Synthesis and Terrestrial Model Inter-comparison Project (MsTMIP) (Huntzinger et al., 2013). Our specific objectives are (1) to attribute the variation in uWUEa to the trend and inter-annual variation (IAV) of the four drivers over the period of 1901–2010, (2) to relate the variation in uWUEa to that in uWUEp and T/ET in response to these drivers, (3) to analyze the spatial variations of the contributions of the four drivers to uWUEa trend, and (4) to diagnose the effects of elevated CO_2 on uWUEa by analyzing the mechanisms regulating the CO_2 effects on uWUEp and T/ET on a global scale.

2. Materials and Methods

2.1. Model Simulations

We used four TBMs, that is, the Community Land Model version 4 (CLM4) (Mao et al., 2012), the CLM4 with surface and subsurface runoff parameterizations from the Variable Infiltration Capacity model (CLM4VIC) (Li et al., 2011), the Dynamic Land Ecosystem Model (DLEM) (Tian et al., 2012), and the Integrated Science Assessment Model (ISAM) (Jain et al., 2009), in MsTMIP to separate the contributions of external drivers to the trend and IAV of uWUEa. All four TBMs include an interactive nitrogen cycle but differ in their treatment of energy, vegetation, carbon, and nitrogen dynamics. This results in different simulated responses of
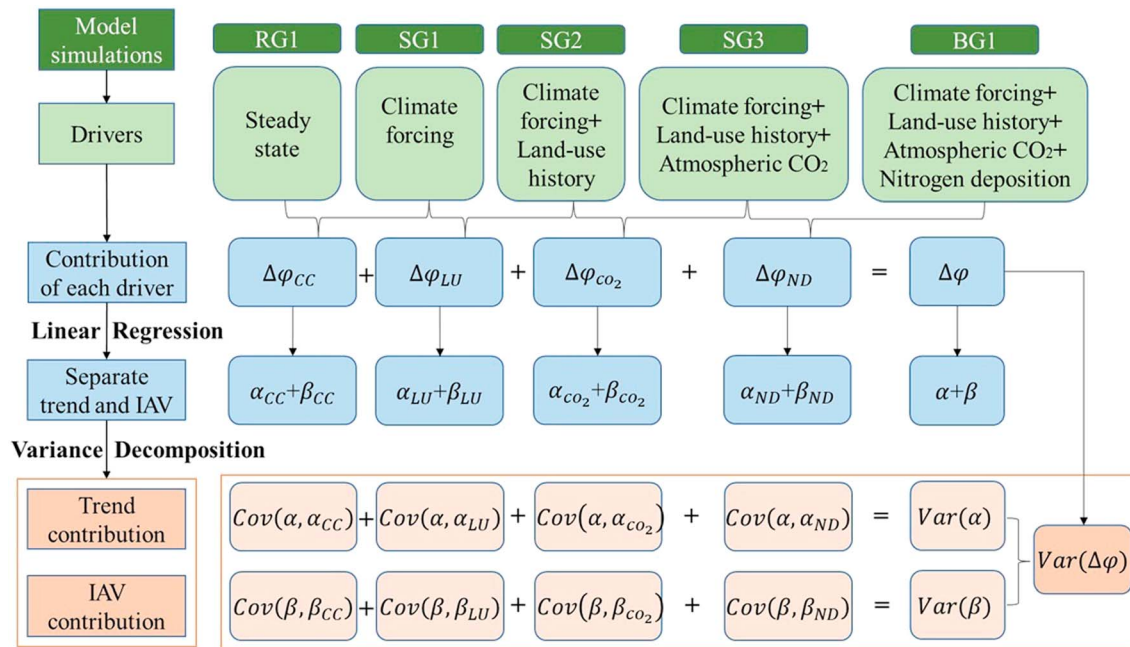
Figure 1. Illustration of the variance decomposition method using model simulations in MsTMIP.

terrestrial ecosystems to changes in external environmental drivers (Huntzinger et al., 2013). The four TBMs were selected because their interactive nitrogen cycle made it possible for them to perform all five simulations in the MsTMIP protocol, which in turn enables a systematic evaluation of model sensitivity to four main external drivers, that is, climate change, land use change, atmospheric CO_2, and nitrogen deposition (Huntzinger et al., 2013). The reference simulation (RG1) was run with steady state environmental forcing (near-preindustrial conditions). The baseline simulation (BG1) was forced by the four drivers. Sensitivity simulations were used to assess the additional impact of each driver, that is, climate change (SG1), land use change (SG2), and atmospheric CO_2 (SG3) sequentially. Therefore, the effects of climate change, land use change, atmospheric CO_2 and nitrogen deposition can be separated as the differences in simulations between SG1 and RG1, SG2 and SG1, SG3 and SG2, and BG1 and SG3, respectively.

In MsTMIP, global simulations were run at the 0.5° × 0.5° spatial resolution and monthly scale from 1901 to 2010 (Huntzinger et al., 2013). The four TBMs share a standardized environmental driver data set, described by Wei et al. (2014). The historical climate forcing (including air temperature, precipitation, downward short-wave and longwave radiation, air specific humidity, pressure, and wind) was obtained from the Climatic Research Unit-National Centers for Environmental Prediction (CRU-NCEP) product (Harris et al., 2014; Kalnay et al., 1996), CO_2 concentration from the extended GLOBALVIEW-CO_2 (GLOBALVIEW-CO_2, 2011), and nitrogen deposition from the global nitrogen deposition data product by Dentener (2006). Land cover and land use change was prescribed by merging the synergetic land cover map (Jung et al., 2006) with the time-varying land use harmonization data in Hurtt et al. (2011), translated by each modeling group into changes in their own maps of vegetation types.

2.2. Attribution Analysis for Annual uWUEa Variation

The joint effect of the four drivers on the annual uWUEa was estimated as the difference in simulated uWUEa between BG1 and RG1 ($\Delta\varphi$). In this study, we have separated the total variation of $\Delta\varphi$ into the variation arising from the trend and IAV for each of the four external drivers over the period of 1901–2010 (Figure 1). Based on five sequential and incremental simulations in MsTMIP, $\Delta\varphi$ can be partitioned into four components, that is, individual effects of climate change ($\Delta\varphi_{CC}$), land use change ($\Delta\varphi_{LU}$), atmospheric CO_2 ($\Delta\varphi_{CO_2}$), and nitrogen deposition ($\Delta\varphi_{ND}$):

$$\Delta\varphi = \Delta\varphi_{CC} + \Delta\varphi_{LU} + \Delta\varphi_{CO_2} + \Delta\varphi_{ND} \qquad (1)$$

where the four components on the right-hand side were calculated as the difference of uWUEa in simulations between SG1 and RG1, SG2 and SG1, SG3 and SG2, and BG1 and SG3, respectively. It is worth noting that the four components in equation (1) represent the incremental effects of the four drivers. For example, $\Delta\varphi_{LU}$ represents the effect of land use change given the climate change represented in SG1. As the full combinations of the four drivers are not considered in the model experimental design in MsTMIP, the interactive effects of these drivers could not be assessed in this study.

A variance decomposition method was used to separate the contributions of the four drivers to the variation in uWUEa. This method is based on the covariance allocation principle for capital allocation, which is widely used for portfolio risk decomposition and attribution (Dhaene et al., 2012). According to the covariance allocation principle, the variance of an aggregate variable can be decomposed into the sum of the covariance between each component variable and the aggregate variable itself (supporting information Text S1). That is, the variance of $\Delta\varphi$, Var($\Delta\varphi$), consists of the covariance between $\Delta\varphi$ and its individual components. The covariance between $\Delta\varphi$ and each driver was further separated into two components: the contribution from the linear trends of the drivers and that from the IAV of the drivers, based on linear regression method (supporting information Text S2). Thus, Var($\Delta\varphi$) is separated into eight components as follows:

$$\mathrm{Var}(\Delta\varphi) = \mathrm{Cov}(\alpha, \alpha_{CC}) + \mathrm{Cov}(\alpha, \alpha_{LU}) + \mathrm{Cov}(\alpha, \alpha_{CO_2}) + \mathrm{Cov}(\alpha, \alpha_{ND}) + \mathrm{Cov}(\beta, \beta_{CC}) + \mathrm{Cov}(\beta, \beta_{LU})$$
$$+ \mathrm{Cov}(\beta, \beta_{CO_2}) + \mathrm{Cov}(\beta, \beta_{ND}) \tag{2}$$

where α and α_{XX} (XX stands for CC, LU, CO$_2$, and ND) represent the linear trend components of the time series of $\Delta\varphi$ and $\Delta\varphi_{XX}$, and β and β_{XX} the IAV components. The covariance terms, that is, Cov(α, α_{XX}) and Cov(β, β_{XX}), represent the contributions from the linear trends of the four drivers, and from the IAV in individual drivers to the variation of $\Delta\varphi$, respectively, over the period of 1901–2010. The relative contribution of each component on the right-hand side of equation (2) is calculated as the ratio of its value and the variance of $\Delta\varphi$. In addition, Var($\Delta\varphi$) can be partitioned into the total trend contribution and the total IAV contribution of $\Delta\varphi$, which is equal to the sum of the four trend components and that of the four IAV components in equation (2), respectively. Thus, the ratio of each trend component over total trend component and that of each IAV component over total IAV component represent the contributions of each driver to the trend and IAV of $\Delta\varphi$, respectively.

2.3. Decomposing the Change in uWUEa Into uWUEp and T/ET

According to Zhou et al. (2016), uWUEa (φ) is expressed as the product of uWUEp (φ_p) by T/ET, that is, $\varphi = \varphi_p \frac{T}{ET}$. Taking RG1 as the reference, the change in φ for BG1 is related to the changes in φ_p and T/ET between the two simulations. According to the total differential of φ, the relative change in φ is approximately decomposed into that in φ_p and T/ET as follows:

$$\frac{\Delta\varphi}{\varphi} \approx \frac{\Delta\varphi_p}{\varphi_p} + \frac{\Delta\left(\frac{T}{ET}\right)}{\frac{T}{ET}} \tag{3}$$

where the symbol Δ represents the change in the variables between BG1 and RG1. Therefore, the contributions of φ_p and T/ET to $\Delta\varphi$ are partitioned as $\frac{\Delta\varphi_p}{\varphi_p}$ and $\frac{\Delta\left(\frac{T}{ET}\right)}{\frac{T}{ET}}$, respectively. In addition, $\frac{\Delta\varphi_p}{\varphi_p}$ and $\frac{\Delta\left(\frac{T}{ET}\right)}{\frac{T}{ET}}$ can be partitioned into eight components as in equation (2), corresponding to the contributions of the linear trends and IAV of the four drivers.

2.4. Quantifying the CO$_2$ Effect on uWUEp and T/ET

The CO$_2$ effect on uWUEa is related to the responses of uWUEp and T/ET to atmospheric CO$_2$, which help understand the variation in uWUEa with rising atmospheric CO$_2$. As indicated by Zhou et al. (2016), ecosystem uWUEp is identical to the uWUE at the leaf scale (φ_i) under steady state conditions, and φ_i is affected by atmospheric CO$_2$ concentrations (Ca) in the form of

$$\varphi_p = \varphi_i = \sqrt{\frac{Ca - \Gamma}{1.6\lambda_{cf}}} \tag{4}$$

where Γ is the leaf CO$_2$ compensation point and the parameter λ_{cf} $(=\frac{\partial T}{\partial A})$ represents the marginal water loss of carbon gain. The equation (4) is derived by combining the carbon and water exchanges through plant stomata and the optimal stomatal conductance model under nonwater stress conditions (Zhou et al., 2016). At the ecosystem scale, λ_{cf} can be derived from φ_p and Ca using equation (4). Atmospheric CO$_2$ impacts φ_p

directly through a combination of its effect on carbon assimilation, and that on transpiration at the leaf scale, the physiological effect on φ_p is therefore estimated by the direct response of φ_p to rising CO_2. According to the optimal stomatal behavior, λ_{cf} remains relatively constant for a given plant but varies with vegetation type (Cowan & Farquhar, 1977; Lloyd, 1991; Lloyd & Farquhar, 1994). For a region with mixed vegetation types, changes in the ecosystem structure, that is, leaf area index (LAI) for different vegetation types, would affect φ_p through changes in λ_{cf}. Thus, the structural effect on φ_p can be evaluated by estimating the change in φ_p in response to changes in λ_{cf} with rising CO_2 at the regional and global scales.

With uWUEp based on SG2 ($\varphi_{p_{SG2}}$) where atmospheric CO_2 is set to be a preindustrial level (284.7 ppm) as the reference, the change in uWUEp for SG3 can be attributed to the effect of atmospheric CO_2 ($\Delta\varphi_{p_{CO_2}}$). The relative change in φ_p between the two simulations can be approximately decomposed into that in $(Ca - \Gamma)$ and λ_{cf} based on the total differential of φ_p in equation (4):

$$\frac{\Delta\varphi_{p_{CO_2}}}{\varphi_{p_{SG2}}} \approx \frac{\Delta(Ca - \Gamma)}{2(Ca - \Gamma)} - \frac{\Delta\lambda_{cf}}{2\lambda_{cf}} \tag{5}$$

where the symbol Δ represents the difference in the variables between SG3 and SG2. The contributions from the physiological effect and the structural effect of CO_2 on $\Delta\varphi_p$ are then separated. The former is evaluated with the relative change in CO_2, and the latter the relative change in λ_{cf}, with a factor of 0.5 corresponding to the radical sign in equation (4).

Atmospheric CO_2 concentration influences T/ET via its effect on T, since ecosystem T decreased by 0.4–5.8 mm with the rising atmospheric CO_2 in SG3, while the increase in canopy interception and soil evaporation was negligible (0–0.3 mm) during the 110 year period (Figure S1 in the supporting information). Thus, the CO_2 effect on T/ET was evaluated by that on T in this study. First, rising atmospheric CO_2 triggers partial stomatal closure (or a decrease in stomatal conductance and hence canopy conductance), resulting in a reduced T per unit leaf area, that is, the physiological effect on T (Medlyn et al., 2001). Second, ecosystem LAI is enhanced by rising atmospheric CO_2, and increased LAI would lead to an increase in ecosystem T, that is, the structural effect on T (Kergoat et al., 2002). The structural effect partially offsets the physiological response of T to rising CO_2. By decomposing T into T/LAI and LAI, the relative change in T is approximately attributed to that in T/LAI and LAI as follows:

$$\frac{\Delta T}{T} \approx \frac{\Delta\left(\frac{T}{LAI}\right)}{\frac{T}{LAI}} + \frac{\Delta LAI}{LAI} \tag{6}$$

Following Beer et al. (2009), T/LAI is approximately expressed as the product of canopy conductance (Gs) of water vapor by VPD, that is, $\frac{T}{LAI} \approx Gs \cdot VPD$, by neglecting the aerodynamic conductance. As VPD is the same for SG2 and SG3, the relative change in T/LAI is equal to that in Gs. The relative change in T between the two simulations is partitioned into that in Gs and in LAI to represent the physiological and structural responses of T to elevated CO_2, respectively. To further assess the sensitivities of T, LAI, and Gs to rising atmospheric CO_2, equation (6) is transformed into

$$\frac{\frac{\Delta T}{T}}{\frac{\Delta Ca}{Ca}} \approx \frac{\frac{\Delta Gs}{Gs}}{\frac{\Delta Ca}{Ca}} + \frac{\frac{\Delta LAI}{LAI}}{\frac{\Delta Ca}{Ca}} \tag{7}$$

The three terms in equation (7) represent the sensitivity coefficients of T, LAI, and Gs to atmospheric CO_2, respectively. Based on the above theoretical analyses, we can better understand the effect of CO_2 on uWUEa by investigating the role of atmospheric CO_2 in uWUEp variations. We can also distinguish the effects of LAI and Gs on T with rising atmospheric CO_2.

2.5. Data Analysis

The monthly outputs of GPP, ET, and T for the five global simulations over the period of 1901–2010 were obtained from each of the four TBMs. VPD was calculated from monthly data of air temperature, pressure, and specific humidity, which were used as the climate forcing for the simulations. To investigate the CO_2 effect on uWUEp and T/ET, the prescribed CO_2 data in MsTMIP were obtained for SG2 and SG3. Since LAI was only available for CLM4 and CLM4VIC, the sensitivity of T to rising atmospheric CO_2 was analyzed based on data from these two models only. The monthly data of air temperature, precipitation, and downward

shortwave radiation obtained from the CRU-NCEP climate forcing were used to analyze the partial correlation between uWUEa and these climate variables in this study.

For the five simulations, monthly GPP, ET, T, and VPD were used as follows: (1) monthly GPP·VPD$^{0.5}$, ET, and T were calculated for each grid cell, and then summed into annual totals; (2) annual GPP·VPD$^{0.5}$, ET, and T were then aggregated into global totals to calculate global annual uWUEa, uWUEp, and T/ET; (3) annual uWUEa, uWUEp, and T/ET were also calculated for each grid cell to evaluate the spatial patterns of their trends using the Theil-Sen regression method (Sen, 1968). In addition, global annual LAI and CO_2 were calculated from monthly data for SG2 and SG3.

The rates of change of these environmental drivers varied with time over the 110 year period (Wei et al., 2014). This may lead to differing rates of change in uWUEa for different periods within the 110 years. Thus, we detected the breakpoints in uWUEa trend using a piecewise linear regression approach (Muggeo, 2003, 2008) to estimate the contributions from the trend and IAV of the environmental drivers to variations in uWUEa during different periods. The R package "segmented" for piecewise linear regression (https://cran.r-project.org/web/packages/segmented/) was used to identify the breakpoint in global annual uWUEa trend for the BG1 simulation.

3. Results

3.1. Responses of uWUEa to the Drivers

Figure 2a shows the time series of the change in global annual uWUEa averaged across the four TBMs due to the effects of the four drivers. For the reference simulation RG1, uWUEa slightly fluctuates without any trend, and its value is 3.49 ± 0.01 g C hPa$^{0.5}$/kg H_2O (mean ± one standard deviation) over the period of 1901–2010 (Figure S2). From the combined effect of the four drivers, uWUEa increased by 0.50 g C hPa$^{0.5}$/kg H_2O, with the effect from atmospheric CO_2, nitrogen deposition, climate change, and land use change of 0.38, 0.12, 0.06, and −0.06 g C hPa$^{0.5}$/kg H_2O, respectively, from the first decade to the last decade (Figure 2a). According to the piecewise linear regression approach, the breakpoint in uWUEa was determined as the year 1975. uWUEa increased by 0.17 g C hPa$^{0.5}$/kg H_2O during the 1901–1975 period (or the first period), with a trend of only 0.02 g C hPa$^{0.5}$/kg H_2O per decade ($p < 0.001$). However, the increasing trend of uWUEa is stronger (0.12 g C hPa$^{0.5}$/kg H_2O per decade, $p < 0.001$) during the 1976–2010 period (or the second period). The large increase in the uWUEa trend was mainly attributed to the higher rate of increase in the atmospheric CO_2 over the second period (Figures 2a and S1).

The effects of the four drivers on uWUEa variation were estimated by separating the relative contribution from the linear trend and that from the IAV of each driver, as shown in Figures 2b and 2c. The four TBMs consistently showed that the trend of rising atmospheric CO_2 played a dominant role ($66 \pm 32\%$) in explaining the uWUEa variation over the 1901–2010 period. The relative contribution of the CO_2 trend was the largest in ISAM (119%) and the smallest in CLM4 and CLM4VIC (42%), indicating large model differences in the effect of CO_2 on uWUEa. During the first and second periods, the CO_2 trend contributed $46 \pm 6\%$ and $64 \pm 32\%$ to the total uWUEa variation, respectively (Figure 2c). The positive trends of nitrogen deposition (ND) and climate change (CC) also contributed to uWUEa variation for the three TBMs ($26 \pm 3\%$ for ND and $10 \pm 1\%$ for CC) except ISAM (both <1%). The trend of land use change produced a large negative contribution (−56%) in ISAM, but its contribution was small in the other three TBMs, ranging from −2.8% to 0.

The relative contributions from the IAV of the four drivers to the variation in uWUEa were relatively small, with a total contribution ranging from only 10% to 37% among the four TBMs over the 110 year period (Figure 2b). In addition, all four TBMs showed that the contributions of the IAV of atmospheric CO_2 and climate change were larger than those of nitrogen deposition and land use change. The climate IAV contributed greatly ($35 \pm 27\%$) to the uWUEa variation over the first period; however, its effect was much smaller ($7 \pm 2\%$) during the second period (Figures 2c and S3). The contributions from the IAV of the other three drivers were much smaller than that of climate over the two periods, indicating that climate variability was the most important driver in determining the IAV of uWUEa. It should be noted that the contribution from the IAV of atmospheric CO_2 was much higher over the full 1901–2010 period than that during the first or second periods. The contribution of the IAV of atmospheric CO_2 was probably overestimated during the 110 year period, because the
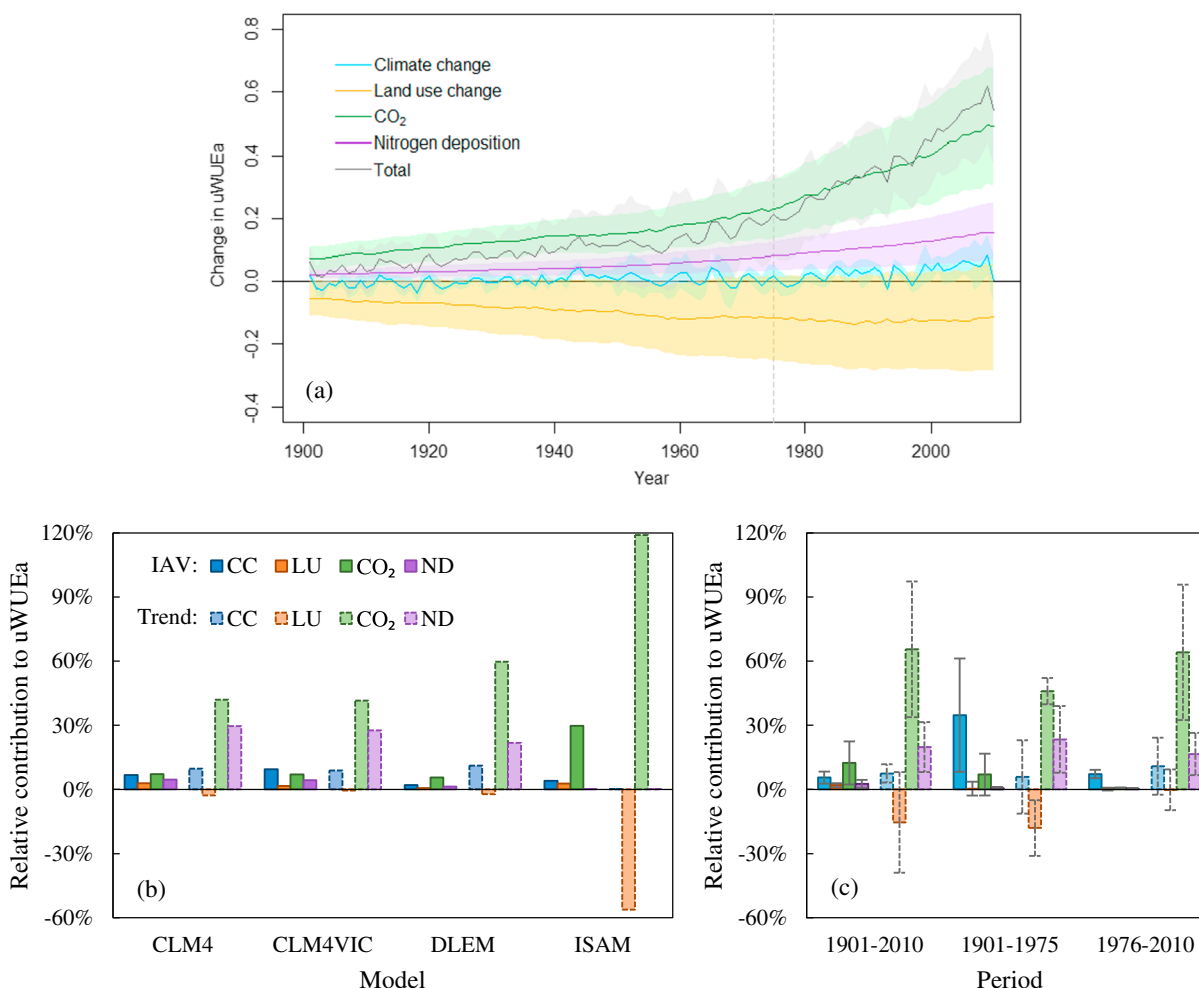
Figure 2. (a) Time series of the change in global annual uWUEa (g C hPa$^{0.5}$/kg H$_2$O) (mean ± one standard deviation) between BG1 and RG1 and its components in correspondence to the four drivers from 1901 to 2010. (b) Relative contributions of the trends and interannual variation (IAV) of the four drivers to the variation in uWUEa for the four TBMs over the period of 1901–2010. (c) Mean contributions of the four TBMs during different periods. The shaded areas in Figure 2a represent one standard deviation in the change of global annual uWUEa across the four models. The error bars in Figure 2c show one standard deviation of the relative contributions over the four TBMs.

trend in atmospheric CO$_2$ changed greatly between the two periods and this change in the rate of increase in CO$_2$ was allocated to the IAV term.

3.2. Changes in uWUEa in Relation to uWUEp and T/ET

The relative change in the uWUEa between BG1 and RG1 was separated into that in uWUEp and T/ET according to equation (3) (Figure 3a). The relative change in uWUEa (5.3 ± 4.3%) during the 110 year period was largely attributed to that in uWUEp (5.9 ± 4.8%), which was slightly offset by the decrease in T/ET (−0.6 ± 0.6%) in response to the four drivers. The increase in uWUEp was mainly attributed to the rising atmospheric CO$_2$, which induced 4.2 ± 1.3% and 11.3 ± 2.4% increase in uWUEp in reference to RG1, across the first and second periods, respectively (Figures 2a and S4). However, the rising atmospheric CO$_2$ led to a slight decrease in T/ET. Nitrogen deposition contributed positively while land use change contributed negatively to the increases in uWUEp and T/ET. Climate change induced relatively small changes in uWUEp and T/ET, which fluctuated between positive and negative values (Figures 3a and S4). Thus, the difference between the contributions of uWUEp and T/ET to uWUEa changes mainly results from their different responses to rising CO$_2$, which will be investigated further.

The relative contributions of the trends and IAV of the four drivers to the changes in uWUEp and T/ET were assessed separately (Figures 3b and 3c and S5). The CO$_2$ trend contributed the most (63.8 ± 25.3%) to the
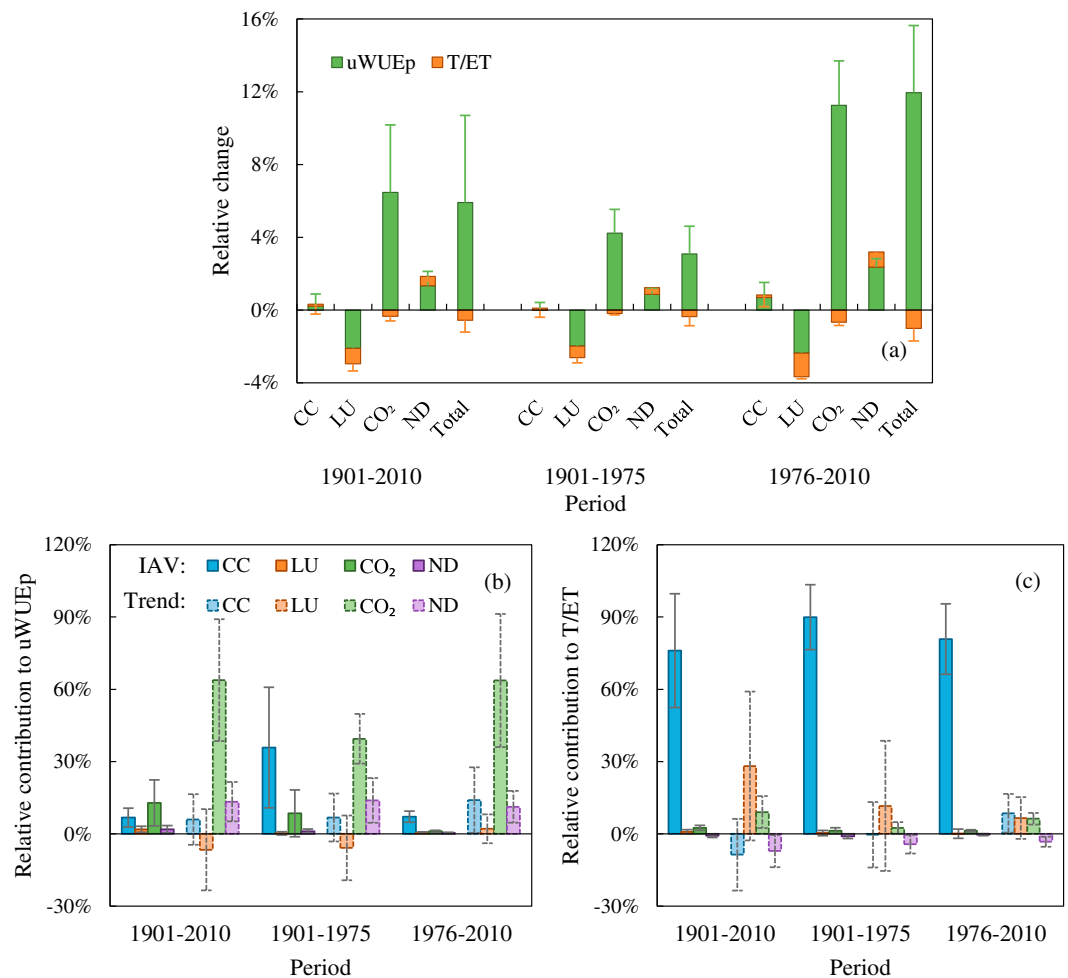
Figure 3. Decomposed relative changes in (a) uWUEp and T/ET in reference to RG1 induced by climate change (CC), land use change (LU), atmospheric CO_2 and nitrogen deposition (ND), and their collective effect during different periods. Relative contributions of the trends and inter-annual variation (IAV) of the four drivers to the change in (b) uWUEp and (c) T/ET during different periods. The error bars in Figure 3a represent one standard derivation for the relative changes across the study period, while the error bars in Figures 3b and 3c represent one standard derivation for the relative contributions across the four models.

change in uWUEp, followed by the nitrogen deposition trend ($13.4 \pm 8.2\%$) over the 110 year period. Climate variability contributed the most among the IAV of the four drivers both during the first ($36 \pm 25\%$) and second ($7 \pm 2\%$) periods. For T/ET, the largest contribution came from climate variability during the first ($90.0 \pm 13.5\%$) and second ($80.9 \pm 14.6\%$) periods, indicating that the change in T/ET was dominated by climate change. During the 1901–2010 period, the trends of atmospheric CO_2 and land use change explained $9.1 \pm 6.6\%$ and $28.2 \pm 30.9\%$ to the change in T/ET, respectively. T/ET was enhanced by nitrogen deposition, and the increasing trend in nitrogen deposition contributed negatively ($-7.2 \pm 6.7\%$) to the change in T/ET. These results indicate that the change in the uWUEa between BG1 and RG1 is dominated by the increasing trend in uWUEp in response to atmospheric CO_2.

3.3. Spatial Variations of the Trend in uWUEa

Figure 4 shows the spatial patterns of the trends of uWUEa in response to climate change, rising atmospheric CO_2, land use change, and nitrogen deposition singly as well as to all four drivers combined over the 1901–1975 and 1976–2010 periods. The positive uWUEa trend during the second period was higher than that for the first period over 79% of the study area. Atmospheric CO_2 alone resulted in an increase of uWUEa for most grid cells (87%), with a larger contribution in the second period than the first period. The effect of nitrogen deposition on the uWUEa trend was much smaller than CO_2, with positive contribution of more than
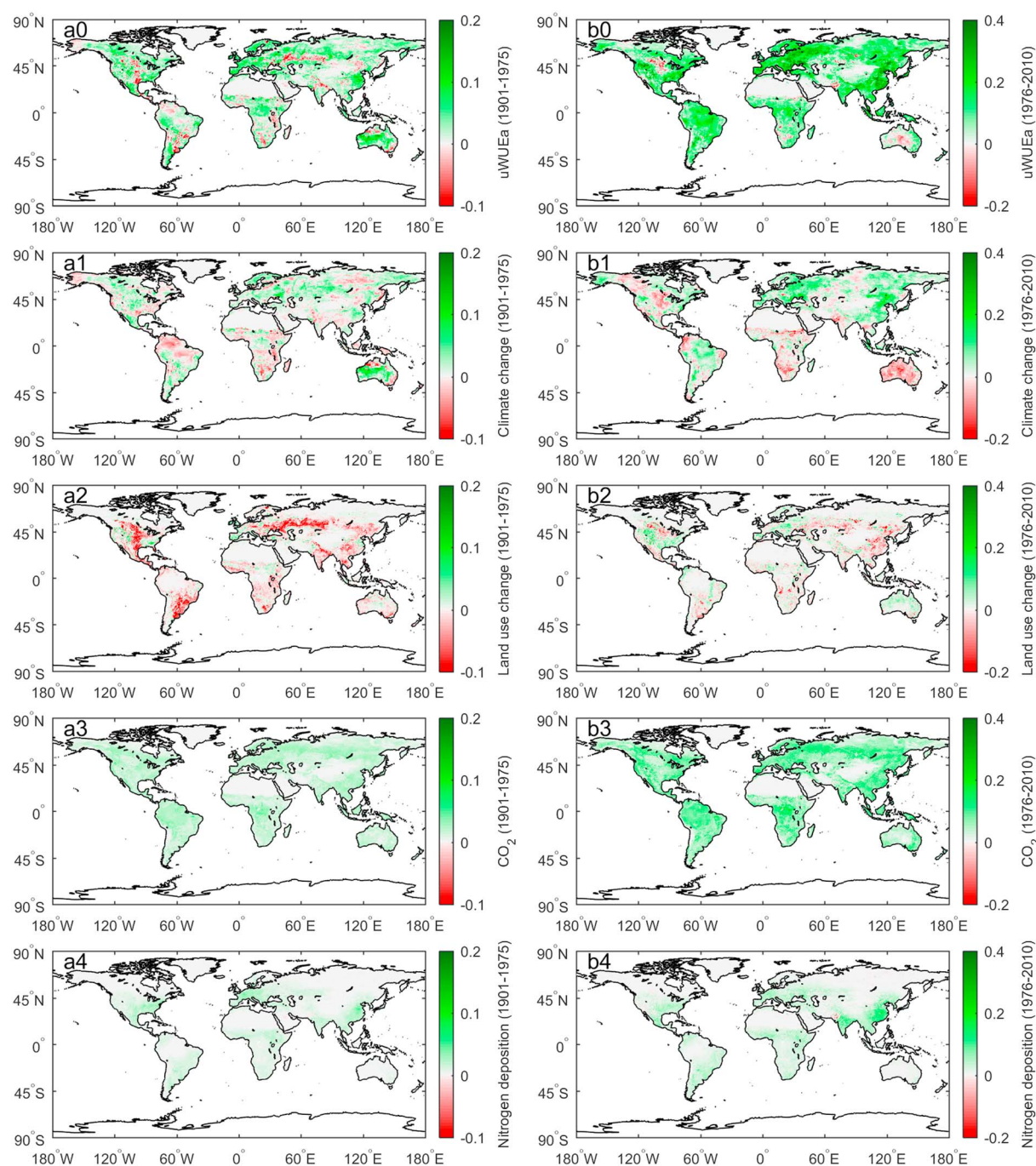
Figure 4. Spatial patterns of the trends of uWUEa (g C hPa$^{0.5}$/kg H$_2$O per decade) and the contributions of the four drivers over the period (a0–a4) 1901–1975 and (b0–b4) 1976–2010. The panels indicate the effects of climate change (Figures 4a1 and 4b1), of land use change (Figures 4a2 and 4b2), of rising CO$_2$ (Figures 4a3 and 4b3), and of nitrogen deposition (Figures 4a4 and 4b4).

0.02 g C hPa$^{0.5}$/kg H$_2$O per decade to the uWUEa trend over 5% of the study area for the first period and 26% of the area for the second period. However, land use change produced a negative effect on uWUEa trend over 48% of the area during the first period, especially in central North America, southeastern Russia, and the southern part of South America. The negative effect of land use change became weaker (37%) during the second period, except for southeastern China. Goldewijk et al. (2011) reported cropland and pasture areas around the world over the last century. Comparing Figures 1 and 2 of Goldewijk et al. (2011), it is evident from Figure 4 of this study that areas with relatively large effects of land use change in Figure 4 of this study

broadly coincide with the global cropland and pasture areas. In addition, the expansion of cropland and pasture occurred more rapidly from 1900 to 1970 than from 1970 to 2000 (Goldewijk et al., 2011), and this period of rapid expansion of the agricultural land is consistent with the larger effect of land use change during the first period than the second period noted in this study. These results show that the increasing trend in uWUEa is mainly ascribed to rising CO_2, followed by nitrogen deposition, and attenuated by land use change at grid scale, and these are consistent with the attribution analysis at the global scale (Figures 2 and 4). Climate change brought about a positive trend in uWUEa in the Northern Hemisphere (NH), but its negative effect was mainly found in the Southern Hemisphere (SH), which explained the relatively small contribution from the trend of climate change to uWUEa variation at the global scale (Figure 4).

The increasing trend of uWUEp was similar to that of uWUEa over the globe, but the spatial variation in uWUEp and T/ET were different, especially during the second period (Figures S6 and S7). Although T/ET increased in most of the NH, it decreased greatly in the SH from 1975 to 2010. These contrasting trends of T/ET were mainly due to climate change, resulting in opposite effects of climate change on uWUEp and uWUEa. It is found that the partial correlation between T/ET and temperature is positive in the NH but largely negative in the SH (Figure S8a). The T/ET increase in the NH and its decrease in the SH suggest that T/ET may respond differently to the increase in temperature in different regions of the world. In addition, the increase in precipitation has contributed to the decrease in T/ET in the Amazon Basin (Figure S8e), where a strong negative correlation between T/ET and precipitation is clearly evident from Figure S8b. The responses of uWUEp and T/ET to atmospheric CO_2 were quite diverse. The CO_2 effect on T/ET was weak around the world over the first period. During the second period, uWUEp increased greatly around the world with rising atmospheric CO_2 concentration, which reduced T/ET at high latitudes (i.e., Alaska, Canada, and northern Eurasia), South America, and Southeast Asia. Both uWUEp and T/ET were slightly enhanced by nitrogen deposition and decreased by land use change, showing similar spatial patterns as the responses of uWUEa.

3.4. CO_2 Effects on uWUEp and T

The CO_2 effects on uWUEp and T were evaluated by comparing SG2 and SG3. Globally, the atmospheric CO_2 concentration in SG3 increased with a trend of 7.6 ppm per decade (Figure S1). Consequently, the CO_2-induced change in uWUEp increased from 0.16 g C $hPa^{0.5}$/kg H_2O during the first decade to 0.96 g C $hPa^{0.5}$/kg H_2O in the last decade at the rate of 0.07 g C $hPa^{0.5}$/kg H_2O per decade. The physiological effect and the structural effect of CO_2 on uWUEp are shown in Figure 5a. The CO_2-induced relative change in uWUEp ranged from 2.3% in 1901 to 17.9% in 2010. However, the direct effect of CO_2 on uWUEp was partially offset by the relative change in the parameter λ_{cf}, which contributed to uWUEp decrease by 0.2%–3.8% during the 110 year period. The increase in λ_{cf} indicated a conversion of vegetation toward less water use efficient types at the global scale with rising CO_2. It was estimated that the physiological effect on uWUEp was reduced by 20 ± 4% (4–24%) through the structural effect from 1901 to 2010 (Figure 5b).

The physiological effect represented by Gs and the structural effect represented by LAI on T in response to rising CO_2 are shown in Figure 5c. The Gs induced decrease in T ranged from 1.8% to 11.3%, while the LAI induced increase in T varied from 1.7% to 9.3%, resulting in a decrease of only 0.2–2.2% during the 110 year period. The relative change in T was strongly correlated with that in atmospheric CO_2 (R^2 = 0.96), with a sensitivity coefficient of −0.06, that is, every 1% increase in atmospheric CO_2 elicited a 0.06% decrease in T (Figure 5d). The CO_2 effect on T is a combination of the positive response of LAI and the negative response of Gs to atmospheric CO_2. LAI and Gs were highly sensitive to atmospheric CO_2 in opposite ways, with every 1% increase in atmospheric CO_2 concentration bringing about a 0.31% increase in LAI (R^2 = 0.97) and 0.37% decrease in Gs (R^2 = 0.99) (Figure 5d). Since the effect of an enhanced LAI growth was moderated by 84% (0.31/0.37) due to the concurrent canopy conductance decrease, the transpiration at the global scale was much less sensitive to CO_2 rise than that at the leaf level.

4. Discussion

4.1. CO_2 Effect on uWUEa Through uWUEp and T

The exchange of carbon and water between terrestrial ecosystems and the atmosphere is affected by rising atmospheric CO_2. At the ecosystem scale, the CO_2 effect on uWUEa can be separated into that of uWUEp and T. The increasing trend of uWUEa throughout the world is ascribed to the strong response of uWUEp to CO_2.
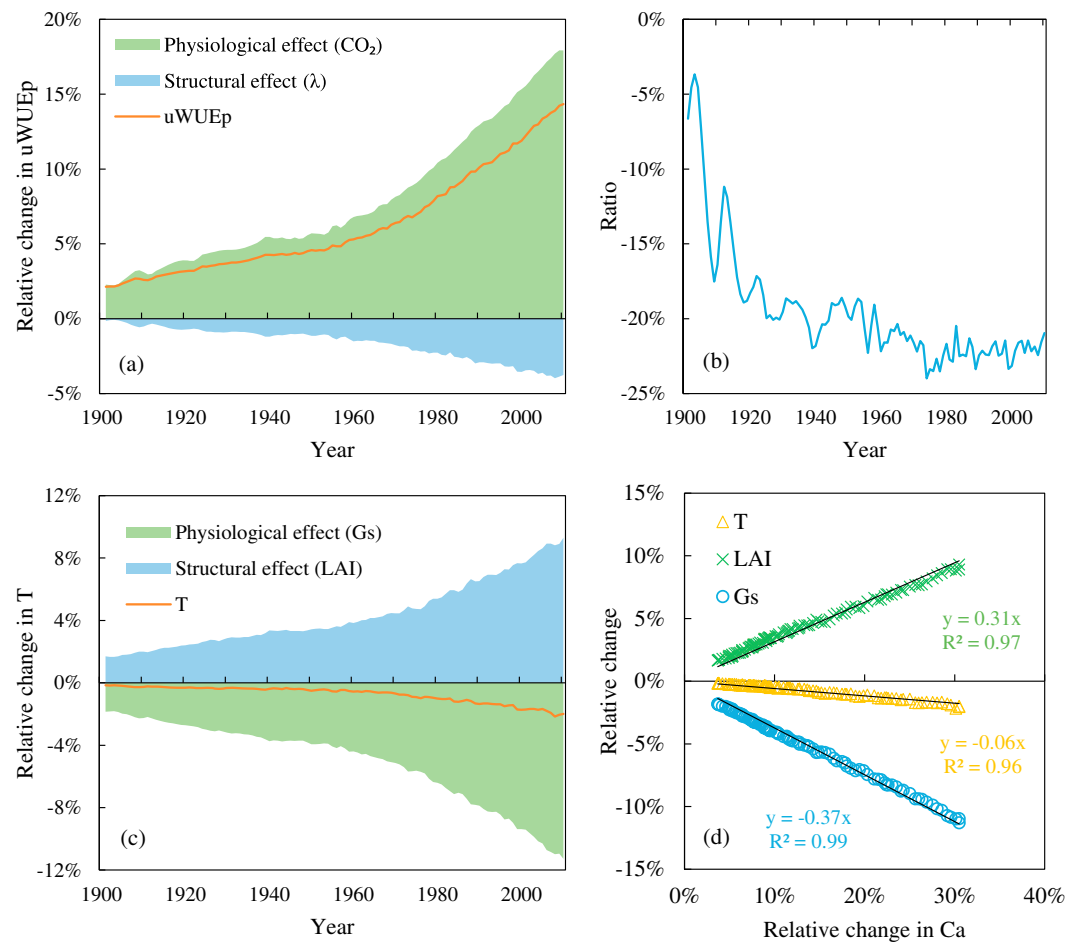
Figure 5. The relative changes in (a) uWUEp and (c) T in response to atmospheric CO_2 (Ca), and the decomposed physiological and structural effects, during the 1901–2010 period. (b) Ratios of the relative change in the parameter λ_{cf} over that in $(Ca - \Gamma)$. (d) Relationships between relative changes in global annual T, LAI, Gs, and the relative change in Ca, respectively.

Ecosystem T is suppressed by rising CO_2 across the world, and its negative effect on uWUEa is much less than the positive effect of uWUEp (Figure 3a). The large difference between the responses of uWUEp and T to atmospheric CO_2 can be explained by their physiological and structural responses to rising CO_2.

Increasing atmospheric CO_2 directly induces physiological changes in plants, that is, reduced stomatal conductance and enhanced carbon assimilation (Ainsworth & Rogers, 2007), resulting in increased uWUE at the leaf level and hence uWUEp at the ecosystem level. The carbon gain is accompanied by leaf area growth, which gives rise to plant canopy change in terrestrial ecosystems to a certain degree (Zhu et al., 2016). Since uWUEp varied with vegetation types, the physiological CO_2 effect on uWUEp may be attenuated or accentuated by ecosystem structural change (e.g., LAI for different vegetation types). Previous studies indicated that changes in vegetation structure partially offset the physiological effect on WUE; thus, WUE may become less responsive to CO_2 at the ecosystem and global scales than at the leaf level (De Kauwe et al., 2013; Knauer et al., 2016). For the first time, this study quantified the contributions of the structural effect and the physiological effect to uWUEp variations at the annual scale from 1901 to 2010. It was estimated that the structural effect has counteracted the physiological effect of atmospheric CO_2 on uWUEp by 20% on average during the 110 year period. In addition, the negative structural effect on uWUEp increase also implied that vegetation types that are less efficient in water use gradually became more dominant around the world with rising CO_2.

The change in ecosystem T in response to rising CO_2 is also jointly determined by the physiological effect through stomatal closure and the structural effect through increase in LAI (Betts et al., 1997; Kergoat et al., 2002). Results from free-air CO_2 enrichment (FACE) experiments showed that stomatal conductance was
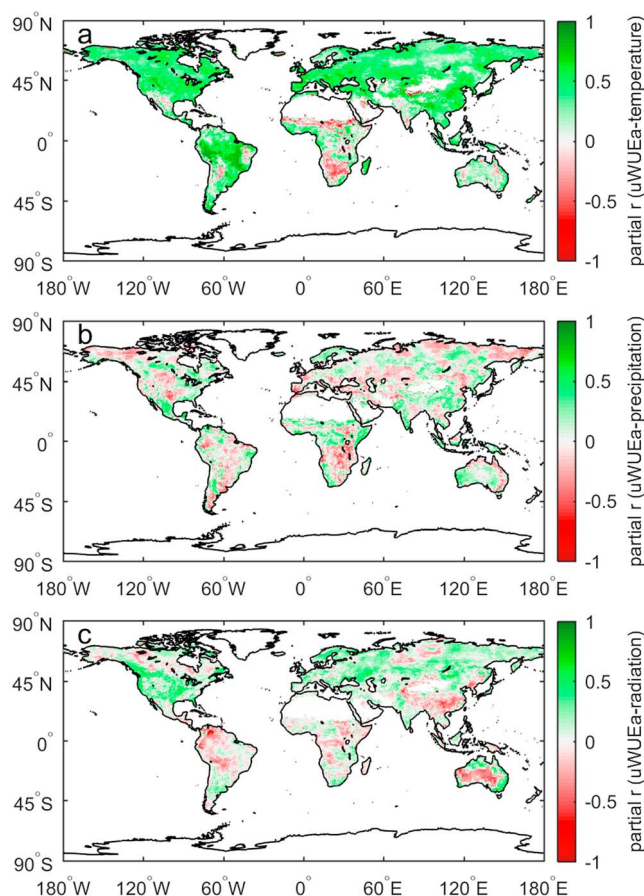
Figure 6. Spatial patterns of partial correlation coefficient (r) between uWUEa and (a) temperature, (b) precipitation, and (c) radiation around each grid cell during the 1901–2010 period.

reduced by 22% on average across all plant species grown at elevated CO_2 (about 155% of ambient level) (Ainsworth & Rogers, 2007), indicating a sensitivity coefficient of 0.4 (22%/55%). The sensitivity coefficient of canopy conductance to increased CO_2 is estimated to be 0.37 at the global level in this study, which is very close to the results from FACE experiments, given the fact that there is minimum constraint on the FACE CO_2 concentrations because of advection. Generally, the sensitivity in the canopy conductance would be lower than that in the stomatal conductance to rising CO_2 when the land surface is not aerodynamically fully coupled to the atmosphere. However, the sensitivity of global T to rising CO_2 is substantially lower than that of canopy conductance as enhanced LAI cancels 84% (0.31/0.37) of water savings caused by stomatal closure, with potential implications for the global hydrological cycle. Pan et al. (2015) and Frank et al. (2015) also suggested small responses of ET and T to increased CO_2, as the stimulated LAI nearly compensated for the effect of stomatal closure.

4.2. Effects of Other Drivers on uWUEa

Based on the variance decomposition method, we found a strong contribution of nitrogen deposition to the trend of uWUEa, just second to the atmospheric CO_2, for all the models except ISAM (Figure 2b). The nitrogen fertilization stimulated both carbon gain and water losses, especially for the nitrogen-limited ecosystems (Lu et al., 2012; Mitchell & Hinckley, 1993). Guerrieri et al. (2016) suggested that ET increased less than GPP with higher canopy nitrogen concentration, resulting in positive correlation between ecosystem WUE and canopy nitrogen concentration at 11 AmeriFlux sites across North America. By comparing SG3 and BG1, we also found that global annual GPP increased by 2.1 ± 1.1% across the four models, while ET only increased by 0.3 ± 0.1%, and uWUEa increased by 1.8 ± 1.0% during 1901–2010 (Figure S9). Overall, the trend and IAV of nitrogen deposition contributed a large proportion (22.4 ± 13.4%) to uWUEa variation over the 1901–2010 period. In addition, the increase in global annual GPP due to nitrogen deposition was greater in CLM4, CLM4VIC, and DLEM than ISAM, resulting in a larger contribution from nitrogen deposition to uWUEa variations. In the first three models, the CO_2 fertilization effect is strongly moderated by nitrogen limitation, so that inclusion of time-varying nitrogen deposition has enhanced its effect on GPP by making more nitrogen available for plant growth.

All of the four models produced positive contributions of the trend and IAV of climate change to uWUEa variation (Figure 2b). Our results indicated that the IAV of uWUEa was mostly attributed to interannual climate variability, that is, the variability of annual temperature, precipitation, and solar radiation, over the two periods. Partial correlation between uWUEa (SG1 with only climate change) and temperature showed that uWUEa was positively correlated with temperature in most area, except for some regions in Africa (Figure 6a). Although ecosystem WUE is expected to decrease due to the enhanced ecosystem ET under climate warming (Niu et al., 2011; Sun et al., 2016), we found that uWUEa increased with warming temperature, which may be due to a temperature-driven increase in VPD. Positive correlation between IWUE and temperature was also observed in the NH and part of the SH during 1982–2008 (Huang et al., 2015). In addition to temperature increase, the increase in solar radiation also contributed to the positive trend of uWUEa in high latitudes, where plant photosynthesis is limited by available solar radiation and positive partial correlation between uWUEa and solar radiation was observed (Figure 6c) (Nemani et al., 2003). The response of uWUEa to precipitation varies among different regions, which may be related to regional climate and vegetation type in the ecosystems (Tian et al., 2010) (Figure 6b). Given the nature of inter-annual variability in precipitation for most regions, the IAV of uWUEa in SG1 was probably attributed to precipitation variability at the global scale.

The contributions of the trend and IAV of land use change to uWUEa variation were estimated to be small at the global scale, except in the model ISAM. By comparison, we found that these different results were attributed to distinctive GPP simulations, for example, in ISAM and CLM4 (Figure S10). The simulated GPP in ISAM was much lower in SG2 with land use change than in SG1. The land use change, however, only led to a small decrease in the simulated GPP in CLM4. In ISAM, the simulated GPP in SG2 was probably influenced by nitrogen limitation, because land use change history can impact the nitrogen status of soils and aboveground biomass (Yang, Richardson, & Jain, 2010). With deforestation for cropland and/or pasture, soil nitrogen was lost due to leaching and higher decomposition rates. A large fraction of biomass nitrogen would be volatilized during clearing and burning of forests. Such nitrogen dynamics with land use change would have significantly reduced available nitrogen for growth, resulting in large decrease in the simulated GPP, especially outside the tropical regions where nitrogen is a limiting nutrient (Jain et al., 2013; Meiyappan et al., 2015). The spatial analysis also indicated that the negative effect of land use change on uWUEa was large in several nontropical regions (Figure 4). However, CLM4 differs from ISAM in several ways. In CLM4, pastures/agricultural regions are represented as natural perennial grasslands (with no grazing or harvest), and these would have GPP nearly as high as forests in the model (Mao et al., 2012). Thus, forest to grass/crop transition may have little impact on GPP for CLM4. In addition, the nitrogen limitation associated with agriculture to forest transition may be underestimated, because agricultural practices that might reduce soil carbon and nitrogen (e.g., tillage and crop harvesting) are not considered in the model. Therefore, the overall impact of land use change on GPP was not large in CLM4.

4.3. The Variance Decomposition Method

In this study, we assessed the individual contributions of the trend and IAV of four external drivers to the variation in uWUEa using a variance decomposition method. This new method is, to our knowledge, applied for the first time to jointly partition the contributions of the trend and IAV components of the drivers together as previous studies performed attribution analysis for the trend and IAV separately (Huang et al., 2015; Zhou et al., 2017). This novel method that provides a simple way for attribution analysis has a great potential for application in both ecology and hydrology.

Using the variance decomposition method, the variance of $\Delta\varphi$ was separated into eight components, based on the covariance of the trend or IAV of $\Delta\varphi$ and its four components, that is, $\Delta\varphi_{CC}$, $\Delta\varphi_{LU}$, $\Delta\varphi_{CO_2}$, and $\Delta\varphi_{ND}$. To partition the trend and IAV components of these variables, we used the linear regression method (Text S2). Thus, the trend term of a variable represented the linear trend over the whole period, and the possible change in the trend during different subperiods was allocated to the IAV term, which may lead to overestimation of the contribution from the IAV of the variable. For example, the contribution of the IAV of $\Delta\varphi_{CO_2}$ to $\Delta\varphi$ variations was overestimated during the 1901–2010 period, because the trend of $\Delta\varphi_{CO_2}$ changed greatly between the 1901–1975 and 1976–2010 periods and this change was allocated to the IAV of $\Delta\varphi_{CO_2}$. Thus, a breakpoint detection procedure, such as the piecewise linear regression approach used in this study, should be applied before using the variance decomposition method to partition the contributions of the trend and IAV components during different subperiods.

4.4. Implications and Limitations of this Study

This study indicates that the trend in uWUEa is mainly attributed to rising atmospheric CO_2 and nitrogen deposition. An in-depth understanding of the responses of uWUEa to rising CO_2 was achieved by theoretically deriving the CO_2 effects on uWUEp and T/ET. Combining the theoretical analysis with model outputs, this study quantitatively estimated the physiological and structural effects of CO_2 on uWUEp and T at the global scale, with implications for future changes in uWUEp and T. Atmospheric CO_2 is predicted to increase toward the end of the 21th century, with an uncertain magnitude associated with emission scenarios (IPCC, 2013). At the same time, nitrogen deposition will continue due to anthropogenic emissions of reactive nitrogen (Liu et al., 2013). The combination of rising CO_2 and nitrogen deposition would greatly enhance carbon gain in terrestrial ecosystems, especially for the nitrogen-limited ecosystems. But their impacts on hydrological processes, that is, T/ET, would not be large because the physiological CO_2 effect on T is almost offset by LAI increases at the global scale. In this study, the response of uWUEp to CO_2 increase is close to that of uWUEa, while the CO_2 induced change in T/ET is an order-of-magnitude smaller. Thus, the magnitude of the uWUEa trend will depend on the responses of uWUEp to rising CO_2 and nitrogen deposition. This

study showed that the physiological CO_2 effect on uWUEp was offset by the structural effect by 4%–24% over the past 110 years (Figure 5b). The CO_2 effect on uWUEp can be easily derived from equation (5), but it is uncertain how much the structural effect will offset the physiological effect on uWUEp in the future, because of the disparate increase in LAI for different vegetation types with a higher atmospheric CO_2.

The main limitation of this study is that the results rely on available model outputs. Models themselves are sources of uncertainty in this assessment. Although the TBMs were not able to fully incorporate processes of global carbon and water cycles for more realistic simulations, they are the only tools available to isolate the effects of external environmental drivers on WUE at the global scale. In addition, the specification of the model scenarios is another source of uncertainty in this study, since the model simulations do not fully account for the interactions between different drivers (Gerber et al., 2013; Yan et al., 2014). It should be noted that the individual effects of the four drivers may be different if we use alternative sequences for sensitivity simulations. For example, the difference between SG2 and SG1 represents the effect of land use change, on the assumption that climate change has occurred. Thus, the interactive effect of climate change and land use change is ascribed to the effect of land use change in this study, not the effect of land use change in isolation under steady state climatic conditions. To account for the interactive effects of the environmental drivers, additional simulations, such as other possible combinations of the external drivers, could also be attempted in future studies.

5. Conclusions

In this study, we proposed a variance decomposition method to attribute the variation in uWUEa to the trends and IAV of four environmental drivers, based on outputs from four terrestrial biosphere models over the period of 1901–2010. The simulated global annual uWUEa was found to increase slowly (0.02 g C hPa$^{0.5}$/kg H_2O per decade) from 1901 to 1975, but quickly (0.12 g C hPa$^{0.5}$/kg H_2O per decade) during 1976–2010. The trend in atmospheric CO_2 contributed the most (66 ± 32%) to the total uWUEa variation, followed by nitrogen deposition and climate change, but the contribution from land use change was negative. Overall, the increasing trend in uWUEa was mostly attributed to the trend in atmospheric CO_2, while the IAV in uWUEa was largely caused by climate variability during the two periods.

uWUEa was partitioned into uWUEp and T/ET to better understand the physiological and structural effects of rising CO_2. The atmospheric CO_2 impacts uWUEp through physiological regulation on carbon assimilation and water transpiration. The physiological effect of CO_2 was offset by 20 ± 4% by the change in ecosystem structure, that is, LAI for different vegetation types, at the global scale, according to the model outputs. However, as much as 84% of the physiological effect on T was canceled by the structural effect (increase in LAI), resulting in only small changes in T/ET under elevated CO_2, indicating that there is little impact of rising CO_2 on hydrological processes. The rising CO_2 will continue to increase uWUEa in future, particularly when combined with nitrogen deposition.

References

Ainsworth, E. A., & Rogers, A. (2007). The response of photosynthesis and stomatal conductance to rising CO_2: Mechanisms and environmental interactions. *Plant, Cell & Environment*, 30(3), 258–270. https://doi.org/10.1111/j.1365-3040.2007.01641.x

Andreu-Hayles, L., Planells, O., GutiÉRrez, E., Muntan, E., Helle, G., Anchukaitis, K. J., & Schleser, G. H. (2011). Long tree-ring chronologies reveal 20th century increases in water-use efficiency but no enhancement of tree growth at five Iberian pine forests. *Global Change Biology*, 17(6), 2095–2112. https://doi.org/10.1111/j.1365-2486.2010.02373.x

Battipaglia, G., Saurer, M., Cherubini, P., Calfapietra, C., McCarthy, H. R., Norby, R. J., & Francesca Cotrufo, M. (2013). Elevated CO_2 increases tree-level intrinsic water use efficiency: Insights from carbon and oxygen isotope analyses in tree rings across three forest FACE sites. *The New Phytologist*, 197(2), 544–554. https://doi.org/10.1111/nph.12044

Beer, C., Ciais, P., Reichstein, M., Baldocchi, D., Law, B. E., Papale, D., … Wohlfahrt, G. (2009). Temporal and among-site variability of inherent water use efficiency at the ecosystem level. *Global Biogeochemical Cycles*, 23, GB2018. https://doi.org/10.1029/2008GB003233

Betts, R. A., Cox, P. M., Lee, S. E., & Ian Woodward, F. (1997). Contrasting physiological and structural vegetation feedbacks in climate change simulations. *Nature*, 387(6635), 796–799. https://doi.org/10.1038/42924

Cowan, I., & Farquhar, G. (1977). Stomatal function in relation to leaf metabolism and environment. *Symposia of the Society for Experimental Biology*, 31, 471–505.

De Kauwe, M. G., Medlyn, B. E., Zaehle, S., Walker, A. P., Dietze, M. C., Hickler, T., … Norby, R. J. (2013). Forest water use and water use efficiency at elevated CO_2: A model-data intercomparison at two contrasting temperate forest FACE sites. *Global Change Biology*, 19(6), 1759–1779. https://doi.org/10.1111/gcb.12164

Dentener, F. J. (2006). Global maps of atmospheric nitrogen deposition, 1860, 1993, and 2050, data set, Oak Ridge National Laboratory Distributed Active Archive Center, Oak Ridge, TN. https://doi.org/10.3334/ORNLDAAC/830, Retrieved from http://daac.ornl.gov/ (last access: 12 April, 2017).

Dhaene, J., Tsanakas, A., Valdez, E. A., & Vanduffel, S. (2012). Optimal capital allocation principles. *The Journal of Risk and Insurance*, *79*(1), 1–28. https://doi.org/10.1111/j.1539-6975.2011.01408.x

Farquhar, G., & Richards, R. (1984). Isotopic composition of plant carbon correlates with water-use efficiency of wheat genotypes. *Functional Plant Biology*, *11*(6), 539–552.

Foley, J. A., DeFries, R., Asner, G. P., Barford, C., Bonan, G., Carpenter, S. R., … Snyder, P. K. (2005). Global consequences of land use. *Science*, *309*(5734), 570–574. https://doi.org/10.1126/science.1111772

Frank, D. C., Poulter, B., Saurer, M., Esper, J., Huntingford, C., Helle, G., … Weigl, M. (2015). Water-use efficiency and transpiration across European forests during the Anthropocene. *Nature Climate Change*, *5*(6), 579–583. https://doi.org/10.1038/nclimate2614

Gagen, M., Finsinger, W., Wagner-Cremer, F., McCarroll, D., Loader, N. J., Robertson, I., … Kirchhefer, A. (2011). Evidence of changing intrinsic water-use efficiency under rising atmospheric CO_2 concentrations in Boreal Fennoscandia from subfossil leaves and tree ring $\delta^{13}C$ ratios. *Global Change Biology*, *17*(2), 1064–1072. https://doi.org/10.1111/j.1365-2486.2010.02273.x

Gerber, S., Hedin, L. O., Keel, S. G., Pacala, S. W., & Shevliakova, E. (2013). Land use change and nitrogen feedbacks constrain the trajectory of the land carbon sink. *Geophysical Research Letters*, *40*, 5218–5222. https://doi.org/10.1002/grl.50957

GLOBALVIEW-CO2 (2011). *Cooperative atmospheric data integration project—Carbon dioxide*, NOAA ESRL, Boulder, CO. Retrieved from http://www.esrl.noaa.gov/gmd/ccgg/globalview/ (last access: 21 April, 2017).

Goldewijk, K. K., Beusen, A., van Drecht, G., & de Vos, M. (2011). The HYDE 3.1 spatially explicit database of human-induced global land-use change over the past 12,000 years. *Global Ecology and Biogeography*, *20*(1), 73–86. https://doi.org/10.1111/j.1466-8238.2010.00587.x

Guerrieri, R., Lepine, L., Asbjornsen, H., Xiao, J., & Ollinger, S. V. (2016). Evapotranspiration and water use efficiency in relation to climate and canopy nitrogen in U.S. forests. *Journal of Geophysical Research: Biogeosciences*, *121*, 2610–2629. https://doi.org/10.1002/2016JG003415

Harris, I., Jones, P. D., Osborn, T. J., & Lister, D. H. (2014). Updated high-resolution grids of monthly climatic observations—The CRU TS3.10 dataset. *International Journal of Climatology*, *34*(3), 623–642. https://doi.org/10.1002/joc.3711

Huang, M. T., Piao, S. L., Sun, Y., Ciais, P., Cheng, L., Mao, J. F., … Wang, Y. P. (2015). Change in terrestrial ecosystem water-use efficiency over the last three decades. *Global Change Biology*, *21*(6), 2366–2378. https://doi.org/10.1111/gcb.12873

Huntzinger, D. N., Schwalm, C., Michalak, A. M., Schaefer, K., King, A. W., Wei, Y., … Zhu, Q. (2013). The North American Carbon Program Multi-Scale Synthesis and Terrestrial Model Intercomparison Project—Part 1: Overview and experimental design. *Geoscientific Model Development*, *6*(6), 2121–2133. https://doi.org/10.5194/gmd-6-2121-2013

Hurtt, G. C., Chini, L. P., Frolking, S., Betts, R. A., Feddema, J., Fischer, G., … Wang, Y. P. (2011). Harmonization of land-use scenarios for the period 1500–2100: 600 years of global gridded annual land-use transitions, wood harvest, and resulting secondary lands. *Climatic Change*, *109*(1-2), 117–161. https://doi.org/10.1007/s10584-011-0153-2

IPCC (2013). In T. F. Stoclker, et al. (Eds.), In *climate change 2013: The physical science basis. Contribution of working group I to the fifth assessment report of the intergovernmental panel on climate change*. Cambridge University Press.

Jain, A., Yang, X., Kheshgi, H., McGuire, A. D., Post, W., & Kicklighter, D. (2009). Nitrogen attenuation of terrestrial carbon cycle response to global environmental factors. *Global Biogeochemical Cycles*, *23*, GB4028. https://doi.org/10.1029/2009GB003519

Jain, A. K., Meiyappan, P., Song, Y., & House, J. I. (2013). CO_2 emissions from land-use change affected more by nitrogen cycle, than by the choice of land-cover data. *Global Change Biology*, *19*(9), 2893–2906. https://doi.org/10.1111/gcb.12207

Jung, M., Henkel, K., Herold, M., & Churkina, G. (2006). Exploiting synergies of global land cover products for carbon cycle modeling. *Remote Sensing of Environment*, *101*(4), 534–553. https://doi.org/10.1016/j.rse.2006.01.020

Kalnay, E., Kanamitsu, M., Kistler, R., Collins, W., Deaven, D., Gandin, L., … Joseph, D. (1996). The NCEP/NCAR 40-year reanalysis project. *Bulletin of the American Meteorological Society*, *77*(3), 437–471. https://doi.org/10.1175/1520-0477(1996)077%3C0437:TNYRP%3E2.0.CO;2

Kaplan, J. O., Krumhardt, K. M., & Zimmermann, N. E. (2012). The effects of land use and climate change on the carbon cycle of Europe over the past 500 years. *Global Change Biology*, *18*(3), 902–914. https://doi.org/10.1111/j.1365-2486.2011.02580.x

Keenan, T. F., Hollinger, D. Y., Bohrer, G., Dragoni, D., Munger, J. W., Schmid, H. P., & Richardson, A. D. (2013). Increase in forest water-use efficiency as atmospheric carbon dioxide concentrations rise. *Nature*, *499*(7458), 324–327. https://doi.org/10.1038/nature12291

Kergoat, L., Lafont, S., Douville, H., & Royer, J.-F. (2002). Impact of doubled CO_2 on global-scale leaf area index and evapotranspiration: Conflicting stomatal conductance and LAI responses, *Journal of Geophysical Research*, *107*(D24), 4808. https://doi.org/10.1029/2001JD001245

Knauer, J., Zaehle, S., Reichstein, M., Medlyn, B. E., Forkel, M., Hagemann, S., & Werner, C. (2016). The response of ecosystem water-use efficiency to rising atmospheric CO_2 concentrations: Sensitivity and large-scale biogeochemical implications. *The New Phytologist*, *213*(4), 1654–1666. https://doi.org/10.1111/nph.14288

Law, B., Falge, E., Gu, L. V., Baldocchi, D., Bakwin, P., Berbigier, P., … Fuentes, J. (2002). Environmental controls over carbon dioxide and water vapor exchange of terrestrial vegetation. *Agricultural and Forest Meteorology*, *113*(1-4), 97–120. https://doi.org/10.1016/S0168-1923(02)00104-1

Levesque, M., Siegwolf, R., Saurer, M., Eilmann, B., & Rigling, A. (2014). Increased water-use efficiency does not lead to enhanced tree growth under xeric and mesic conditions. *The New Phytologist*, *203*(1), 94–109. https://doi.org/10.1111/nph.12772

Li, H., Huang, M., Wigmosta, M. S., Ke, Y., Coleman, A. M., Leung, L. R., … Ricciuto, D. M. (2011). Evaluating runoff simulations from the Community Land Model 4.0 using observations from flux towers and a mountainous watershed. *Journal of Geophysical Research*, *116*(D24), D24120. https://doi.org/10.1029/2011JD016276

Liu, X., Zhang, Y., Han, W., Tang, A., Shen, J., Cui, Z., … Zhang, F. (2013). Enhanced nitrogen deposition over China. *Nature*, *494*(7438), 459–462. https://doi.org/10.1038/nature11917

Lloyd, J. (1991). Modelling stomatal responses to environment in Macadamia integrifolia. *Functional Plant Biology*, *18*(6), 649–660.

Lloyd, J., & Farquhar, G. D. (1994). 13C discrimination during CO_2 assimilation by the terrestrial biosphere. *Oecologia*, *99*(3-4), 201–215. https://doi.org/10.1007/BF00627732

Lu, C., Tian, H., Liu, M., Ren, W., Xu, X., Chen, G., & Zhang, C. (2012). Effect of nitrogen deposition on China's terrestrial carbon uptake in the context of multifactor environmental changes. *Ecological Applications*, *22*(1), 53–75. https://doi.org/10.1890/10-1685.1

Mao, J., Thornton, P. E., Shi, X., Zhao, M., & Post, W. M. (2012). Remote sensing evaluation of CLM4 GPP for the period 2000–2009. *Journal of Climate*, *25*(15), 5327–5342. https://doi.org/10.1175/jcli-d-11-00401.1

Matson, P., Lohse, K. A., & Hall, S. J. (2002). The globalization of nitrogen deposition: Consequences for terrestrial ecosystems. *Ambio*, *31*(2), 113–119. https://doi.org/10.1579/0044-7447-31.2.113

Medlyn, B. E., Barton, C. V. M., Broadmeadow, M. S. J., Ceulemans, R., De Angelis, P., Forstreuter, M., … Jarvis, P. G. (2001). Stomatal conductance of forest species after long-term exposure to elevated CO_2 concentration: A synthesis. *The New Phytologist*, *149*(2), 247–264. https://doi.org/10.1046/j.1469-8137.2001.00028.x

Meiyappan, P., Jain, A. K., & House, J. I. (2015). Increased influence of nitrogen limitation on CO_2 emissions from future land use and land use change. *Global Biogeochemical Cycles*, *29*, 1524–1548. https://doi.org/10.1002/2015GB005086

Mitchell, A., & Hinckley, T. (1993). Effects of foliar nitrogen concentration on photosynthesis and water use efficiency in Douglas-fir. *Tree Physiology*, *12*(4), 403–410. https://doi.org/10.1093/treephys/12.4.403

Muggeo, V. M. (2003). Estimating regression models with unknown break-points. *Statistics in Medicine*, *22*(19), 3055–3071. https://doi.org/10.1002/sim.1545

Muggeo, V. M. (2008). Segmented: An R package to fit regression models with broken-line relationships. *R news*, *8*(1), 20–25.

Nemani, R. R., Keeling, C. D., Hashimoto, H., Jolly, W. M., Piper, S. C., Tucker, C. J., … Running, S. W. (2003). Climate-driven increases in global terrestrial net primary production from 1982 to 1999. *Science*, *300*(5625), 1560–1563. https://doi.org/10.1126/science.1082750

Niu, S., Xing, X., Zhang, Z. H. E., Xia, J., Zhou, X., Song, B., … Wan, S. (2011). Water-use efficiency in response to climate change: From leaf to ecosystem in a temperate steppe. *Global Change Biology*, *17*(2), 1073–1082. https://doi.org/10.1111/j.1365-2486.2010.02280.x

Nock, C. A., Baker, P. J., Wanek, W., Leis, A., Grabner, M., Bunyavejchewin, S., & Hietz, P. (2011). Long-term increases in intrinsic water-use efficiency do not lead to increased stem growth in a tropical monsoon forest in western Thailand. *Global Change Biology*, *17*(2), 1049–1063. https://doi.org/10.1111/j.1365-2486.2010.02222.x

Osmond, C., Bjorkman, O., & Anderson, D. (1980). *Physiological processes in plant ecology: Toward a synthesis with Atriplex* (pp. 1–468). Berlin: Springer. https://doi.org/10.1007/978-3-642-67637-6

Pan, S., Tian, H., Dangal, S. R. S., Yang, Q., Yang, J., Lu, C., … Ouyang, Z. (2015). Responses of global terrestrial evapotranspiration to climate change and increasing atmospheric CO_2 in the 21st century. *Earth's Future*, *3*(1), 15–35. https://doi.org/10.1002/2014ef000263

Peñuelas, J., Canadell, J. G., & Ogaya, R. (2011). Increased water-use efficiency during the 20th century did not translate into enhanced tree growth. *Global Ecology and Biogeography*, *20*(4), 597–608. https://doi.org/10.1111/j.1466-8238.2010.00608.x

Piao, S., Friedlingstein, P., Ciais, P., de Noblet-Ducoudre, N., Labat, D., & Zaehle, S. (2007). Changes in climate and land use have a larger direct impact than rising CO_2 on global river runoff trends. *Proceedings of the National Academy of Sciences of the United States of America*, *104*(39), 15,242–15,247. https://doi.org/10.1073/pnas.0707213104

Saurer, M., Spahni, R., Frank, D. C., Joos, F., Leuenberger, M., Loader, N. J., … Young, G. H. (2014). Spatial variability and temporal trends in water-use efficiency of European forests. *Global Change Biology*, *20*(12), 3700–3712. https://doi.org/10.1111/gcb.12717

Sen, P. K. (1968). Estimates of the regression coefficient based on Kendall's tau. *Journal of the American Statistical Association*, *63*(324), 1379–1389. https://doi.org/10.1080/01621459.1968.10480934

Sterling, S. M., Ducharne, A., & Polcher, J. (2013). The impact of global land-cover change on the terrestrial water cycle. *Nature Climate Change*, *3*(4), 385–390.

Sun, Y., Piao, S., Huang, M., Ciais, P., Zeng, Z., Cheng, L., … Zeng, H. (2016). Global patterns and climate drivers of water-use efficiency in terrestrial ecosystems deduced from satellite-based datasets and carbon cycle models. *Global Ecology and Biogeography*, *25*(3), 311–323. https://doi.org/10.1111/geb.12411

Tian, H., Chen, G., Liu, M., Zhang, C., Sun, G., Lu, C., … Chappelka, A. (2010). Model estimates of net primary productivity, evapotranspiration, and water use efficiency in the terrestrial ecosystems of the southern United States during 1895-2007. *Forest Ecology and Management*, *259*(7), 1311–1327. https://doi.org/10.1016/j.foreco.2009.10.009

Tian, H., Chen, G., Zhang, C., Liu, M., Sun, G., Chappelka, A., … Vance, E. (2012). Century-scale responses of ecosystem carbon storage and flux to multiple environmental changes in the southern United States. *Ecosystems*, *15*(4), 674–694. https://doi.org/10.1007/s10021-012-9539-x

Wei, Y., Liu, S., Huntzinger, D. N., Michalak, A. M., Viovy, N., Post, W. M., … Shi, X. (2014). The North American Carbon Program Multi-scale Synthesis and Terrestrial Model Intercomparison Project—Part 2: Environmental driver data. *Geoscientific Model Development*, *7*(6), 2875–2893. https://doi.org/10.5194/gmd-7-2875-2014

Yan, J., Zhang, D., Liu, J., & Zhou, G. (2014). Interactions between CO_2 enhancement and N addition on net primary productivity and water-use efficiency in a mesocosm with multiple subtropical tree species. *Global Change Biology*, *20*(7), 2230–2239. https://doi.org/10.1111/gcb.12501

Yang, X., Richardson, T., & Jain, A. (2010). Contributions of secondary forest and nitrogen dynamics to terrestrial carbon uptake. *Biogeosciences*, *7*(10), 3041–3050. https://doi.org/10.5194/bg-7-3041-2010

Zhou, S., Yu, B., Huang, Y., & Wang, G. (2014). The effect of vapor pressure deficit on water use efficiency at the subdaily time scale. *Geophysical Research Letters*, *41*, 5005–5013. https://doi.org/10.1002/2014GL060741

Zhou, S., Yu, B., Huang, Y., & Wang, G. (2015). Daily underlying water use efficiency for AmeriFlux sites. *Journal of Geophysical Research – Biogeosciences*, *120*(5), 887–902. https://doi.org/10.1002/2015JG002947

Zhou, S., Yu, B., Zhang, Y., Huang, Y., & Wang, G. (2016). Partitioning evapotranspiration based on the concept of underlying water use efficiency. *Water Resources Research*, *52*(2), 1160–1175. https://doi.org/10.1002/2015WR017766

Zhou, S., Zhang, Y., Ciais, P., Xiao, X., Luo, Y., Caylor, K. K., … Wang, G. (2017). Dominant role of plant physiology in trend and variability of gross primary productivity in North America. *Scientific Reports*, *7*, 41366. https://doi.org/10.1038/srep41366

Zhu, Q., Jiang, H., Peng, C., Liu, J., Wei, X., Fang, X., … Yu, S. (2011). Evaluating the effects of future climate change and elevated CO_2 on the water use efficiency in terrestrial ecosystems of China. *Ecological Modelling*, *222*(14), 2414–2429. https://doi.org/10.1016/j.ecolmodel.2010.09.035

Zhu, Z., Piao, S., Myneni, R. B., Huang, M., Zeng, Z., Canadell, J. G., … Zeng, N. (2016). Greening of the Earth and its drivers. *Nature Climate Change*, *6*(8), 791–795. https://doi.org/10.1038/nclimate3004